THE CRAMER-RAO BOUND FOR POLE AND AMPLITUDE ESTIMATES OF DAMPED EXPONENTIAL SIGNALS IN NOISE †

William M. Steedly **Randolph L. Moses**

ElectroScience Laboratory
Department of Electrical Engineering
The Ohio State University, Columbus, Ohio 43210

Abstract

This paper extends the CRB derivation in [1] to the case where signals consist of arbitrary exponential terms in noise. Expressions for the CRBs of the parameters of an exponential model with one set of poles and multiple sets of amplitude coefficients are derived. The poles of this model are not constrained and may lie anywhere in the complex plane. The results of the paper provide a complete description of the CRB of pole estimates for arbitrary exponential signals in noise.

I. Introduction

The problem of estimating model parameters of noisy exponential signals is an active area of research. The performance of these parameter estimation methods is often measured by the accuracy of the estimated poles, since these pole locations contain such information as formant frequencies or directions of arrival of signal components. This problem is considered in [1], and estimators are derived for the case where the poles are confined to lie on the unit circle. To evaluate the accuracy of the estimators, a general expression for the Cramer-Rao Bound (CRB) is derived for the angles of the estimated poles under the assumption that the poles of the signal lie on the unit circle.

This paper extends the CRB derivation in [1] to the case where the signal consists of arbitrary exponential terms. In this extension, the poles of the signal may lie anywhere in the complex plane. An expression of the CRB is derived for both the angles and the magnitudes of the poles, and for the amplitudes associated with these poles. This work can also be seen as an extension of the CRB expressions developed in [2].

Using these expressions, this paper then compares pole estimation accuracy as functions of pole magnitude, data length, and pole separation. It is shown that for small data lengths, poles slightly inside the unit circle are more accurately estimated than poles on the unit circle. In addition, the transition from the $1/m^3$ (where m is the number of data points) variance bounds decrease for poles on the unit circle to the variance decrease as poles move off the unit circle is also detailed.

†This research was supported in part by the Air Force Office of Scientific Research, Bolling AFB, DC

II. The Cramer-Rao Bound Derivation

A. Data Model

Assume we have N "snapshots" of data vectors $y(t)$, each of length m:

$$y(t) = \begin{bmatrix} y_0(t) & y_1(t) & \cdots & y_{m-1}(t) \end{bmatrix}^T \quad t = 1, 2, \ldots, N.$$

Each data vector is modeled as a noisy exponential sequence

$$y_q(t) = \sum_{i=1}^{n} x_i(t) p_i^q + e_q(t) \quad q = 0, 1, \ldots, m-1. \quad (1)$$

There are n exponential modes in the data; the n poles $\{p_i\}_{i=1}^n$ do not vary from snapshot to snapshot, but the amplitudes $x_i(t)$ may vary.

Equation (1) may be compactly written as

$$y(t) = A(p)x(t) + e(t), \quad (2)$$

where the noise vector $e(t)$ is given by,

$$e(t) = \begin{bmatrix} e_0(t) & e_1(t) & \cdots & e_{m-1}(t) \end{bmatrix}^T,$$

the amplitude vector $x(t)$ is given by

$$x(t) = \begin{bmatrix} x_0(t) & x_1(t) & \cdots & x_{m-1}(t) \end{bmatrix}^T,$$

and A is the $m \times n$ Vandermonde matrix derived from n signal poles, $\{p_i\}$

$$A = \begin{bmatrix} 1 & 1 & \cdots & 1 \\ p_1 & p_2 & \cdots & p_n \\ p_1^2 & p_2^2 & \cdots & p_n^2 \\ \vdots & \vdots & & \vdots \\ p_1^{m-1} & p_2^{m-1} & \cdots & p_n^{m-1} \end{bmatrix}. \quad (3)$$

Here, it is assumed that the $e(t)$ are uncorrelated zero mean white Gaussian noise vectors with variance σ.

CH2977-7/91/0000-3569 $1.00 © 1991 IEEE

B. CRB Covariance Matrix

From equation (2), the likelihood function of the data is given by

$$L(y(1),\ldots,y(N)) = \frac{1}{(\pi\sigma)^{mN}} \times \exp\left\{-\frac{1}{\sigma}\sum_{t=1}^{N}[y(t)-Ax(t)]^H[y(t)-Ax(t)]\right\}.$$

Thus, the log-likelihood function is

$$\ln(L) = -mN\ln(\pi) - mN\ln(\sigma) - \frac{1}{\sigma}\sum_{t=1}^{N}[y^H(t)-x^H(t)A^H][y(t)-Ax(t)]. \quad (4)$$

We define α_i and ω_i to be the magnitude and angle of each pole p_i, thus $p_i = \alpha_i e^{j\omega_i}$.

Define the parameter vector θ as

$$\theta = \begin{bmatrix} \sigma & M^T & \omega_1 & \cdots & \omega_n & \alpha_1 & \cdots & \alpha_n \end{bmatrix}^T,$$

where M is a vector containing the real and imaginary components of the amplitudes:

$$M = \begin{bmatrix} \bar{x}^T(1) & \tilde{x}^T(1) & \cdots & \bar{x}^T(N) & \tilde{x}^T(N) \end{bmatrix}^T,$$

where $\bar{x}(t) = \mathrm{Re}\{x(t)\}$ and $\tilde{x}(t) = \mathrm{Im}\{x(t)\}$.

From the partial derivatives of equation (4) with respect to σ, $\{\bar{x}(t)\}$, $\{\tilde{x}(t)\}$, $\{\omega_i\}$, and $\{\alpha_i\}$, the Fisher information matrix is found to be

$$I_\theta = \begin{bmatrix} \frac{mN}{\sigma^2} & & & & & & & \\ & \bar{H} & -\tilde{H} & & & & \bar{\Delta}_{\omega 1} & \bar{\Delta}_{\alpha 1} \\ & \tilde{H} & \bar{H} & & & & \tilde{\Delta}_{\omega 1} & \tilde{\Delta}_{\alpha 1} \\ & & & \ddots & & & \vdots & \vdots \\ & & & & \bar{H} & -\tilde{H} & \bar{\Delta}_{\omega N} & \bar{\Delta}_{\alpha N} \\ & & & & \tilde{H} & \bar{H} & \tilde{\Delta}_{\omega N} & \tilde{\Delta}_{\alpha N} \\ & \bar{\Delta}_{\omega 1}^T & \tilde{\Delta}_{\omega 1}^T & \cdots & \bar{\Delta}_{\omega N}^T & \tilde{\Delta}_{\omega N}^T & \Gamma_\omega & \Gamma_{\omega\alpha} \\ & \bar{\Delta}_{\alpha 1}^T & \tilde{\Delta}_{\alpha 1}^T & \cdots & \bar{\Delta}_{\alpha N}^T & \tilde{\Delta}_{\alpha N}^T & \Gamma_{\omega\alpha}^T & \Gamma_\alpha \end{bmatrix},$$

where

$$\begin{aligned} H &= \frac{2}{\sigma}A^H A \\ \Delta_{\omega k} &= \frac{2}{\sigma}A^H D_\omega X(k) \\ \Delta_{\alpha k} &= \frac{2}{\sigma}A^H D_\alpha X(k) \\ \Gamma_\omega &= \frac{2}{\sigma}\sum_{t=1}^{N}\mathrm{Re}\{X^H(t)D_\omega^H D_\omega X(t)\} \\ \Gamma_{\omega\alpha} &= \frac{2}{\sigma}\sum_{t=1}^{N}\mathrm{Re}\{X^H(t)D_\omega^H D_\alpha X(t)\} \\ \Gamma_\alpha &= \frac{2}{\sigma}\sum_{t=1}^{N}\mathrm{Re}\{X^H(t)D_\alpha^H D_\alpha X(t)\}. \end{aligned}$$

Each $X(t)$ is a diagonal matrix given by

$$X(t) = \begin{bmatrix} x_1(t) & & \bigcirc \\ & \ddots & \\ \bigcirc & & x_n(t) \end{bmatrix}$$

and D_ω and D_α are matrices obtained by differentiating each element in $A(p)$ (see equation (3)) with respect to its pole angle and magnitude, respectively.

For a given model, the Fisher information matrix I_θ can be inverted to provide the CRB covariance matrix for the parameters σ, $\{\bar{x}(t)\}$, $\{\tilde{x}(t)\}$, $\{\omega_i\}$, and $\{\alpha_i\}$.

C. CRB Covariance Matrix for Pole Angle and Pole Magnitude Only

In many cases one is interested only in the behavior of the pole magnitudes and angles. For this case, we define

$$\theta_1 = \begin{bmatrix} \omega_1 & \omega_2 & \cdots & \omega_n & \alpha_1 & \alpha_2 & \cdots & \alpha_n \end{bmatrix}^T.$$

Then the CRB for θ_1 is found using partial inverse of a partitioned matrix and given by

$$\mathrm{CRB}_{\theta_1} = \left(\begin{bmatrix} \Gamma_\omega & \Gamma_{\omega\alpha} \\ \Gamma_{\omega\alpha}^T & \Gamma_\alpha \end{bmatrix} - \sum_{t=1}^{N}\mathrm{Re}\left\{\begin{bmatrix} \Delta_{\omega t}^H G \Delta_{\omega t} & \Delta_{\omega t}^H G \Delta_{\alpha t} \\ \Delta_{\alpha t}^H G \Delta_{\omega t} & \Delta_{\alpha t}^H G \Delta_{\alpha t} \end{bmatrix}\right\}\right)^{-1},$$

where $G \equiv H^{-1}$.

Note that one can also obtain the CRB for the pole accuracy in terms of its real and imaginary parts by a simple Jacobian coordinate transformation of CRB_{θ_1}.

III. Examples and Observations

This section presents examples which illustrate the behavior of pole CRBs with respect to pole magnitude, data length, and pole separation.

A. Pole Magnitude and Data Length

In this simulation, a model with a single pole and with one snapshot of data was chosen. The amplitude coefficient associated with the pole was chosen such that the signal energy was unity. The noise power was also kept constant at $\sigma = 1$.

The CRBs for the pole angle and magnitude appear in Figures 1 and 2, respectively for various pole magnitudes and various data lengths. From Figure 1 we see that the pole angle CRB is (logarithmically) symmetric with respect to the unit circle. The pole magnitude variance (Figure 2) is not symmetric, and smallest at a pole radius less than one. If we normalize these bounds by the square of the pole magnitude, the magnitude variance becomes log-symmetric.

The CRBs for both pole angle and magnitude are asymptotically lowest when the pole is on the unit circle, and that on the unit circle the CRB is decreasing by $1/m^2$ (m is the data length). This is consistent with the well-known $1/m^3$ variance decrease, since the amplitude coefficient was varied in this experiment in order to keep the energy constant. Note, however, that as the number of data points is reduced, the pole magnitude which gives the minimum CRB is less than unity.

Note also that the decrease in the CRB as m is increased is limited when the pole is off the unit circle and that the maximum decrease is smaller when the pole is further away from the unit circle. This corresponds to high decay/growth rates which result in significantly large data points only at one end of the set or the other, making additional data points insignificant.

B. Angle Separation

In this simulation we consider two poles at $\alpha_1 e^{j\Delta\omega/2}$ and $\alpha_2 e^{-j\Delta\omega/2}$ for various data lengths and angle separation $\Delta\omega$. Again, $\sigma = 1$ and each amplitude is chosen such that the mode energy is unity. Figure 3 shows the CRB for the angle of each pole versus pole angle separation when $\alpha_1 = \alpha_2 = 1$ (i.e. both poles are on the unit circle). The CRBs for the pole magnitudes are equal to the pole angle CRBs because these poles are located on the unit circle. These results are consistent with [3].

Figure 4 shows the angle CRBs for pole 1 when $\alpha_1 = .85$ and $\alpha_2 = .95$. The CRBs for pole 2 have a similar shape, but are lower for the larger data lengths. The CRBs for each pole magnitude are proportional to the angle CRBs.

The bounds in Figure 4 exhibit the same type of characteristics as in Figure 3. One major difference, however, is the fact that as $\Delta\omega \rightarrow 0$ the CRBs remain finite in Figure 4. This is due to the fact that the poles are at different radii. For large $\Delta\omega$ and larger m the variances are higher in Figure 4 than in Figure 3; this is expected in light of the single pole results.

C. Amplitude Coefficient CRBs

Inversion of the Fisher information matrix I_θ gives the CRBs for the amplitude coefficients as well as the poles.

As an example, Figure 5 shows the CRBs for the amplitude coefficient real part for the previous single pole example. The CRB results for the amplitude coefficient imaginary part are identical to those for the real part. The sharp decrease in the curves as the pole magnitude becomes greater than 1 is due to the sharp decrease in the values of the amplitude needed to keep the mode energy equal to one.

D. Pole Error Ellipses

The CRB gives the variance bound for the pole magnitude, angle, and also the cross correlation between the two. These can be used to generate an error ellipse around each pole. As an example, Figure 6 is a plot of the 2 standard deviation error ellipses for ten poles each with mode energy equal to one, using $m = 100$ data points and $\sigma = .1$. Note that all of the ellipses are circles, indicating that real and imaginary parts of the pole error are uncorrelated. This is the case in all examples tested to date, but no general proof of this property has been found.

IV. Conclusions

We have derived expressions for the CRBs of the parameters of an exponential model with one set of poles and multiple sets of amplitude coefficients. The poles of this model may lie anywhere in the complex plane. The CRB for pole angle is log-symmetric about the unit circle with minimum on the unit circle, while the CRB for pole magnitude has its minimum inside the unit circle for finite length data sets and is not symmetric. Simulation results have also shown that error standard deviation ellipses about poles turn out to be circular. The CRBs for estimates of the amplitude coefficients in terms real and imaginary parts are also available.

References

[1] P. Stoica and A. Nehorai, "MUSIC, maximum likelihood, and Cramer-Rao bound," *IEEE Transactions on Acoustics, Speech, and Signal Processing*, vol. ASSP–37, pp. 720–741, May 1989.

[2] R. Kumaresan and D. W. Tufts, "Estimating the parameters of exponentially damped sinusoids and pole-zero modeling in noise," *IEEE Transactions on Acoustics, Speech, and Signal Processing*, vol. ASSP-30, pp. 833–840, Dec. 1982.

[3] D. C. Rife and R. R. Boorstyn, "Multiple tone parameter estimation from discrete-time observations," *Bell System Technical Journal*, vol. 55, pp. 1389–1410, Nov. 1976.

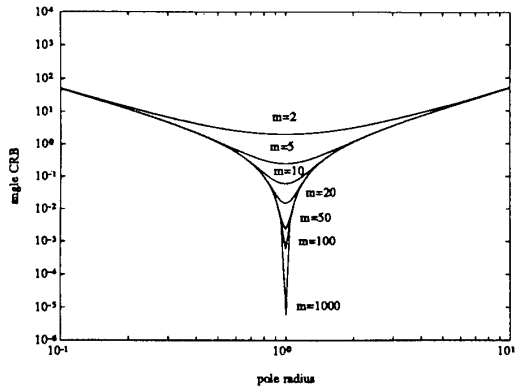

Figure 1: Pole angle CRBs.

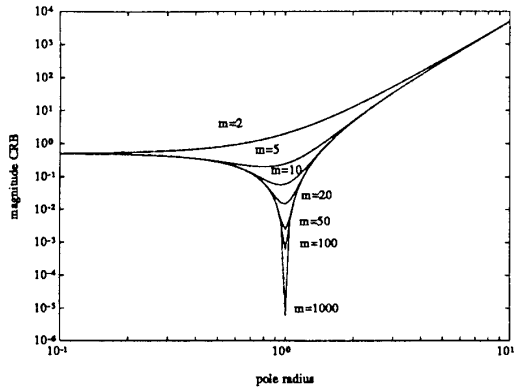

Figure 2: Pole magnitude CRBs.

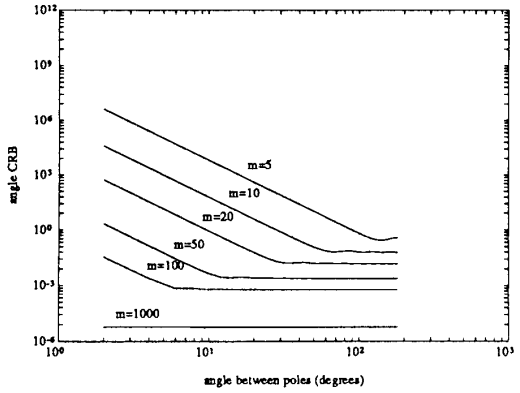

Figure 3: Angle CRB as a function of pole separation.

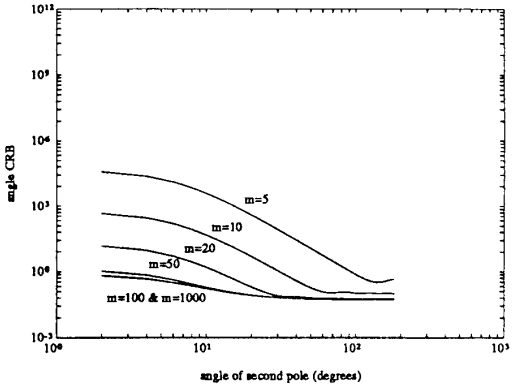

Figure 4: Pole angle CRBs for p_1.

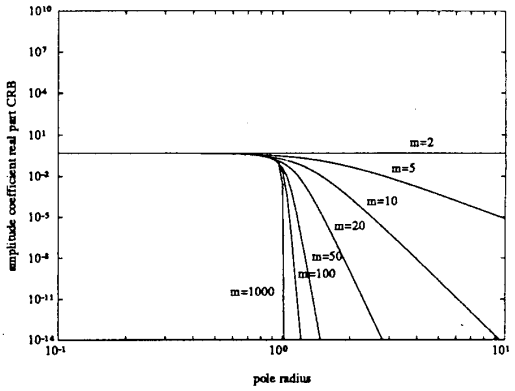

Figure 5: Amplitude coefficient real part CRBs.

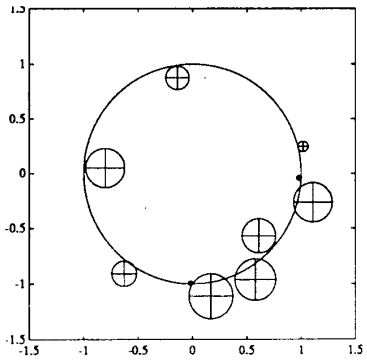

Figure 6: Standard deviation circles for a tenth order model.